Study of the possibility to use a RADAR in a dedicated mission to explore the Pioneer anomaly

Report of Denis Defrère's training period performed in the Advanced Concepts Team (ESTEC-ESA)

European Space Agency
Advanced Concepts Team

University of Liege
Faculty of Applied Sciences

Supervised by
A. Rathke and J. P. Swings

Academic year
$2004 - 2005$

Contents

Chapter 1

Introduction

1.1 General information about ESTEC

The European Space and Technology Center (ESTEC) is the largest research centre of ESA, the European Space Agency. ESTEC is located in Noordwijk, near Amsterdam in the Netherlands. Most of the activities at ESTEC consist in developing a space project and looking at the feasibility of ideas.

Figure 1.1: XMM assembly and testing at ESTEC.

Another important task for the ESTEC specialists it to work closely together with European Space industries in developing and testing the technologies needed to make future projects possible. Many laboratories and service facilities in different fields of expertise are hosted and available not only to the Agency itself but also to external customers. In 2004, the upper and lower modules of the ESA's X-ray Multi-Mirror (XMM) was in one of the ESTEC's cleanrooms for the structural and thermal model in preparation for the alignment, vibration and acoustic testing (see Fig. 1.1). During my training period, I had the chance to see the Automated Transfer Vehicle (ATV) which will be launched this year to supply the international space station in experimental equipment and spare parts as food, air and water for its permanent crew.

The headquarters of ESA is in Paris where the policies and programmes are decided upon. However, ESA also has other centres in Europe, each of which has different responsibilities.

- The European Space Operations Centre (ESOC). It is responsible for controlling ESA satellites in orbit and is situated in Darmstadt, Germany.

- The European Astronauts Centre (EAC). It is the astronauts training centre for future missions and it is situated in Cologne, Germany.

- The European Space Research Institute (ESRIN). It is based in Frascati, near Rome in Italy. Its responsibilities include collecting, storing and distributing satellite data to ESA's partners, and acting as the Agency's information technology centre.

In addition, ESA has liaison offices in Belgium, the United States and Russia; a launch base in French Guiana; and ground and tracking stations in various areas of the world. In February 2005, the total number of staff working for ESA numbered approximately 1907.

ESA's mandatory activities are funded by a financial contribution from all the 16 Agency's Member States, calculated in accordance with each country's gross national product. Moreover, ESA conducts a number of optional programmes. Individual countries decide in which optional programme they wish to participate and the amount they wish to contribute. For 2005, ESA's budget is 2977 million of euros. The agency operates on the basis of geographical return, i.e. it invests in each Member State, through industrial contracts for space programmes, an amount more or less equivalent to each country's contribution. European per capita investment in space is very little. On average, every citizen of an ESA Member State pays, in taxes for expenditure on space, about the same as the price of a cinema ticket. In the United States, investment in civilian space activities is almost four times as much.

The ESA Council is the Agency's governing body and provides the basic policy guidelines within which the Agency develops the European space programme. Each Member State is represented on the council and has one vote, regardless of its size or financial contribution. The agency is headed by a Director General, elected by the Council every four years. Each individual research sector has its own Directorate that reports to the Director General.

1.2   The Advanced Concepts Team

From the first of February till the end of April, I have performed a training period at ESTEC in the Advanced Concept Team (ACT)[1]. ACT is part of the ESA's Advanced Concepts and Studies Office, or DG-X, in the Agency's Directorate General. The main purposes of DG-X are the management of the Agency's General Studies Programme and the assessment of new working methods and mission concepts.

The main objective of ACT is to enhance cooperation with Universities and Research Institutes working on advanced research topics and its application to space systems. The team consist mainly in Ph.D. who have a contract for 1 or 2 years and have each their own field of research. The main fields are

- Space solar power
- Advanced power systems
- Trajectory design and optimisation
- Advanced propulsion
- Fundamentals physics
- Biomimicry
- Mathematics and informatics
- Planetary protection

and other topics in which both space systems engineering competence and specific theoretical knowledge are required. During my training period, I was supervised by Andreas Rathke, the responsible for the fundamentals physics field.

---

[1]http://www.esa.int/gsp/ACT/about.htm

1.3   Training period's objectives

In preparation of a one-day workshop at ESTEC with the Pioneer anomaly community, I was assigned to study the radar option for accurate range measurements in a first dedicated mission to the Pioneer anomaly. The mission consists essentially of a mother craft, which will track a subsatellite by means of laser or radar. The concept of the mission is illustrated in the figure below.
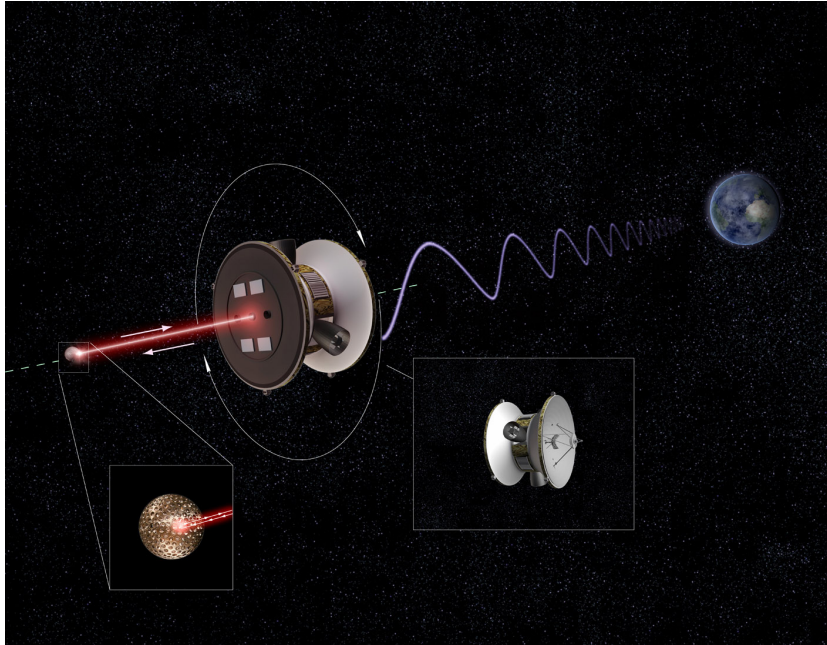

Figure 1.2: Formation flight scenario: an active spacecraft tracking a locally detached, formation flying reference inertial masses via ranging and angular sensors. The spheres have been previously released from the spacecraft.

To measure the position of the subsatellite, the first idea was to use a laser tracking system. However, since the subsatellite will be very small and located at roughly 1 km from the mother craft, the laser beam will be very hard to accommodate in the good direction. The problem could be solved by using a radar tracking system. Considering the upcoming technologies, my task was to determine if it could be relevant for the mission. In particular, the main constraint was to find a radar system which can achieve appropriate angular and distance resolutions with a minimum consumption in power.

Few days before the workshop, two of the main authors on the Pioneer anomaly , S.G. Turishev[2] and M.M. Nieto[3] came to ESTEC in order to define the specifications of the mission. I was invited to take part to discussions and to give my results. The way to reconstruct the subsatellite's orbit, by minimizing the errors introduced by the motion of the mother craft, was also intensively discussed. This was very interesting since many aspects of a mission was discussed and illustrated with values corresponding to present and future technologies.

In the following, the present status of the mission is first briefly described before giving the study of the radar option. Then, the results of the workshop are given in chapter 4.

---

[2]Jet Propulsion Laboratory, Pasadena CA, USA.
[3]Los Alamos National Laboratory (LANL), Los Alamos NM, USA.

Chapter 2

A Mission to Explore the Pioneer Anomaly

2.1 The Pioneer missions and the anomaly

The Pioneer 10/11 missions, launched on 2 March 1972 (Pioneer 10) and 5 April 1973 (Pioneer 11), were the first to explore the outer solar system. After Jupiter and (for Pioneer 11) Saturn encounters, the two spacecraft followed escape hyperbolic orbits near the plane of the ecliptic to opposite sides of the Solar System. The Pioneers were excellent craft to perform accurate celestial mechanics experiments and are still the most precisely navigated deep space vehicles. This is due to a combination of many factors.

1. The attitude control. The spin-stabilization are such as a minimum number of commanded attitude correction maneuvers are required.

2. The power design. The power sources, the Radioisotope Thermoelectric Generators (RTGs), are built with enlarged radiation fins and situated on extended booms, aided the stability of the craft and also reduced the heat systematics.

3. The precise Doppler tracking. A sensitivity to resolve small frequency biases and drifts at the level of mHz/s was achieved.

By 1980, Pioneer 10 had passed a distance of ~ 20 astronomical units (AU) from the Sun and the acceleration contribution from solar-radiation pressure on the craft (directed away from the Sun) had decreased to less than 4×10^{-8} cm/s^2. At that time an anomaly in the Doppler signal became evident. Subsequent analysis of the radio-metric tracking data from both the Pioneer 10 and Pioneer 11 spacecraft at distances between 20-70 AU from the Sun, on opposite sides of the Solar System, has consistently indicated the presence of an anomalous, small, constant Doppler frequency drift for both craft. The drift can be interpreted as being due to a constant acceleration of $a^* = (8.74 \pm 1.33) \times 10^{-10}$ m/s^2 directed towards the Sun [1, 2, 3] or to a blueshift in the frequency of light.

Although the most obvious explanation would be that there is a systematic origin to the effect, perhaps generated by the spacecraft themselves from excessive heat or propulsive gas leaks, none has been found; that is, no unambiguous, onboard systematic has been discovered [1, 2, 4]. In fact, attempts to find a convincing explanation using such a mechanism have not been successful. This inability to explain the anomalous acceleration of the Pioneer spacecraft with conventional physics has contributed to the growing discussion about its origin.

2.2   Objectives for a mission to explore the anomaly

The anomaly is unambiguously present in the Pioneer Doppler tracking data. However, it is still unexplained. Referring to the extensive efforts that have gone into its investigation, it seems unlikely that the cause of the anomaly can be found from solely the Pioneer data. In the same manner, the other deep-space spacecraft (Voyager, Galileo, Ulysses, and Cassini) are not suitable to study the anomaly because their navigational data have all their own individual difficulties for use in an independent test [5, 6]. In addition, many of the deep-space missions that are currently being planned either will not provide the needed navigational accuracy and trajectory stability of under 10^{-10} m/s^2 (i.e., Rosetta, New Horizons, Interstellar Probe) or else they will have significant on-board systematics that mask the anomaly (i.e., JIMO - Jupiter Icy Moons Orbiter). Hence a new dedicated space experiment will be necessary to determine the nature of the Pioneer Anomaly. In fact, there is a significant international effort to support development of a dedicated mission to study the anomalous signal. In particular, in 2004 the Centre of Applied Space Technology and Microgravity (ZARM) of the University of Bremen, Germany organized an international workshop to study "The Pioneer Anomaly and Mission Proposals to Test It." This and two follow-up gatherings have resulted in this consolidated European-US proposal for an ESA Cosmic Vision Theme for the period 2015-2025.

The main objective of the proposed mission is to identify the origin of the anomalous Doppler frequency drift exhibited by the radio tracking of the Pioneer spacecraft with an accuracy of at least three orders of magnitude below the inferred size of the anomaly. This objective translates into the following science and technology requirements:

1. For precise trajectory determination, the mission shall achieve navigational and attitude reconstruction accuracy at the level of $\sim 0.01 \times 10^{-8}$ cm/s^2 with emphasis on the effects of small constant (i.e. DC) accelerations.

2. For precise proper time monitoring, the mission shall achieve a clock acceleration resolution at the level of 3×10^{-21} for clocks positioned either on-board of the spacecraft or on the ground.

These goals translate into requirements on the spacecraft design that require technologies and instrumental solutions capable of detecting, monitoring, and compensating for small forces that affect a spacecraft's motion and communication signal in the deep space. In particular, the acceleration regime in which the anomaly was observed diminishes the value of using modern disturbance compensation systems developed for other fundamental physics and formation flying experiments. For example, the systems that are currently being developed for the LISA (Laser Interferometric Space Antenna) and LISA Pathfinder missions are designed to operate in the presence of a low frequency acceleration noise (at the mHz level), while the Pioneer anomalous acceleration is a strong constant bias in the Doppler frequency data. In addition, currently available DC accelerometers are a few orders of magnitude less sensitive than is needed for a test. Furthermore, should the anomaly be a force that universally affects frequency standards [3], the use of accelerometers would shed no light on what is the true nature of the observed anomaly. Nevertheless, the use of accelerometers might useful to discriminate against the effects due to well-known non-gravitational forces acting on the spacecraft while in the deep space.

Independently of the science outcome, the initiated technology development might also be an important result of the proposed mission. Future precision experiments in very deep space are currently being envisioned. As is vividly demonstrated by the Pioneers, the effects of small systematic forces are not easily modeled and compensated for, even today. Further, communication frequency drifts are generally not monitored at the required level and, in fact, these levels are a few orders below the desired sensitivity. Therefore, understanding the anomaly would benefit

the design of more stable and less noisy spacecraft. In conclusion the outcome of a space mission to investigate the Pioneer anomaly will be twofold: It will help in understanding the laws of nature and it will provide the technology that enables new, even more precise space experiments to investigate them.

In the next section, we discuss the mission design features for a proposed deep-space experiment to explore the Pioneer anomalous signal. The mission is designed to determine the origin of the discovered anomaly, and to characterize its properties to an accuracy of at least three orders of magnitude below the size of the anomaly. It will be able to determine if the anomaly is due to some unknown physics or else to an on-board systematic. Either way the result would be of major significance. If the anomaly is a manifestation of new or unexpected physics, the result would be of truly fundamental importance. However, if the anomaly turns out to be an unknown manifestation of an on-board spacecraft systematic, its understanding would radically affect the design of future precision space navigation, especially in deep space.

2.3 Mission's concepts

In this Section, we described the baseline concept of a future mission aimed at testing the Pioneer anomaly by using existing spacecraft technologies in combination with newly developed capabilities.

2.3.1 Formation flying technologies

Development of precision formation flying (PFF) technologies had become one of the top priorities for both ESA and NASA. In particular, the recent NASA Research Announcement calls for development of PFF as the enabling technology to meet the near future high priority science objectives. Due to limitations of launch vehicle fairing sizes and of the ability to phase optical elements over long distances on flexible structures, separated spacecraft formation flying is the only viable means to satisfy many demands of modern astronomy and fundamental physics. Therefore, as a baseline design, it is chosen a concept that relies on the precision formation flying and which does not have to cancel or limit systematics because there are essentially no significant systematics present. The design has a primary craft that is robust and able to nurture itself for 7-12 years in the environment of deep space (see Fig. 2.1 below). The craft would communicate high-precision Doppler and range data to Earth, with X- or Ka-band, or perhaps even via optical communication.
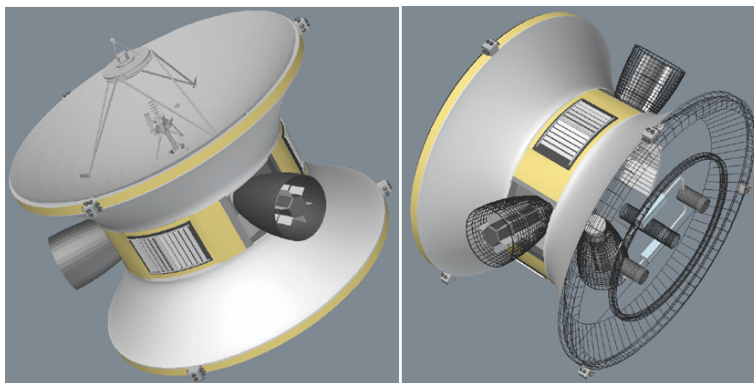

Figure 2.1: Current design of the spacecraft.

The Pioneer lessons should lead to a spacecraft design that allows a sufficiently precise discrimination of non-gravitational forces affecting the motion of a probe in the deep space. The proposed design relies on the symmetry of the spacecraft (both inertial and thermal), shielding or/and active disturbance compensation; continuity of the measurements, as well as accurate simulation of the environment affecting the spacecraft.

Concept description

Formation flight can avoid the inherent problems of self disturbance of an inertial sensor on board the primary spacecraft by placing the inertial reference mass (i.e. subsatellite) outside the craft at a sufficient, but not too large distance. Laser ranging sensor that employ a milli-W laser monitors the 3-dimensional vector of mutual separation between the spacecraft and the subsatellite. The subsatellite is covered with cornercube retro-reflectors that enable precise laser ranging similar to the current satellite and lunar laser ranging methods. For the radar tracking, the subsatellite must be as reflective as possible in order to maximize the returning power. Fig. 2.2 shows a generic concept.
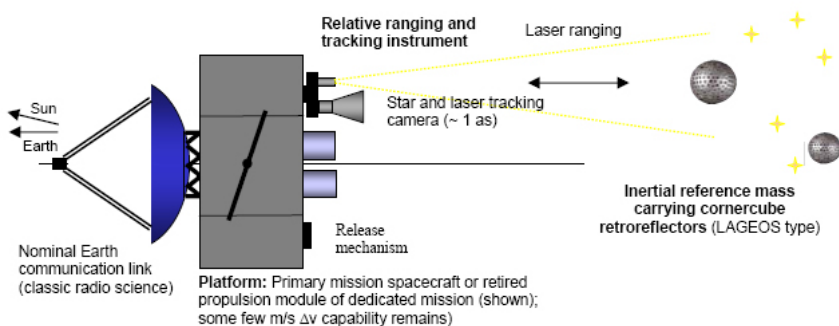

Figure 2.2: Formation flight scenario: an active spacecraft tracking a locally detached, formation flying reference inertial masses via ranging and angular sensors. The spheres have been previously gently released from the spacecraft. Additional on-board sensors may include magnetometer, solar radiation intensity monitors, and a dust spectrometer including both charge and inertial sensors [7].

To enable this concept three requirements must be fulfilled:

1. The subsatellite must be at a sufficient distance from the main craft so that any radiant heat from the primary craft will not affect the motion of the subsatellite.

2. For the purposes of not causing a significant force on the subsatellite, the reflected signal must be modeled to high accuracy.

3. The primary craft must be able to perform the ranging to determine the relative position history for the subsatellite. This mean that the primary craft will be able to follow the subsatellite in a formation flight.

The objective of this architecture is to precisely measure the motion of the inertial reference mass and to eliminate the effect of any disturbance of the primary spacecraft on the subsatellite. Conceptually, a combination of two observables related to the precise distance determination between the Earth and the spacecraft and between the spacecraft and the subsatellite would yield even more accurate distance between the Earth and the subsatellite. The spacecraft does not have to be dynamically quiet as long as the relative distance and lateral position remain within the tracking capability. The current estimates suggest tolerable distances up to few km

with a lateral imbalance of up to 5 degrees. The advantage of this scenario is that the distance to the inertial reference mass is decoupled from the design and performance characteristics of the primary spacecraft.

The spacecraft has to provide a few Δv capability throughout the mission and an accurate release mechanism for the reference masses. It does not need to perform large maneuvers. Further, the relative range, range rate and lateral tracking is a 3-dimensional two-step process and needs to be sufficiently accurate in relative angle determination between main link to Earth and local link to reference.

2.3.2 Mass and power budgets

Presently the only source of autonomous power in the deep space is the use of RTGs. About 50-75 W of electrical power are needed to run the communications and heat the fuel (for maneuvering). Since the electrical thermocouples degrade with time, the power at launch should be of order 140 W. Since RTG efficiencies are of order 6-7%, one would end up with at least 2000 W of thermal power from the RTGs.

Assuming some technological advances in the near future, the following mass budget is envisioned : The RTGs will weigh about 55 kg per kW of power produced. The spacecraft bus, including the inertial release mechanism, thermal insulation and radio system with a standard Cassegrain antenna will be of order 45 kg. The propulsion system, with both the attitude control and a small ΔV capability, is about 35 kg. The laser system will add 25 kg to the total mass (20 kg for the radar system), so as the stable clock on-board of the primary spacecraft. Addition of a star tracker with a μrad accuracy would add up to 5 kg. All in all we are talking of a craft of ~ 200 kg. The subsatellite with a diameter of ~ 10 cm, covered with a silica retroreflectors, will result in an about 8 kg of extra weight. Thus, despite the apparent advantages, the mission operation has some added complexity. Thus, the dedicated payload, including reference masses, could be in the range of 150-300 kg.

2.3.3 Mission operations

The proposed mission concept will validate the capability of multiple spacecraft flying in formation to minimize effect of the small non-gravitational forces affecting their trajectory. The separation distances during normal operations may vary between 100 m and 3 km. In addition, the interspacecraft range, inertial attitude, and estimation/control will be performed on-board and implemented through cross links. The formation operations will be designed so as to minimize fuel consumption needed for formation keeping. Formation control will employ low thrust actuation devices on the spacecraft. Moreover, control will be autonomous and collaborative among the spacecraft, with no ground intervention. Finally, full six degree-of-freedom formation control will be performed.

The mission is divided into two phases, which will require significantly different operations. The boost phase will require monitoring of the mission trajectory. The type and intensity of the required operations will depend on the selected mechanism for the acceleration. For chemical propulsion with planetary gravity assists maneuvers, a regular monitoring of the trajectory will suffice. This will be interleaved with short intense operations periods for the steering during planetary fly-bys. In the other cases where more continuous propulsion is applied, such as solar sailing or solar electric based propulsion systems, a more active monitoring and correcting are to be expected during cruise.

In order to simplify the corrections, spacecraft maneuvers shall be minimized to those absolutely necessary, the study will indicate, depending on the mission profile, if accurate tracking during maneuvers will be necessary.

During the propulsion phase, telemetry will be mainly used for the housekeeping information of the propulsion system. A downlink capability of ~ 1 Kbps would be convenient. The required telemetry capability for the measurement phase depends on the additional instrumentation. Consumption for range and range rate is negligible, and then very limited housekeeping is required. An additional accelerometer would require a few Kbps.

During the measurement phase the system should operate autonomously. Precision ranging and range rate measurements will be performed at regular intervals. Initially a number of 1000 measurement points was assumed over a period of about 4-5 years. This results in about one measurement per month.

2.3.4 Communications and navigation budgets

The communication system should enable determination of the Earth-spacecraft distance with an accuracy of less then 1 m and a range rate resolution at the level of ~ 1 $\mu m/s$ over the 40 AU range. To simplify the spacecraft geometry and the effects of environmental forces, the communication system will utilize a small high-gain antenna of ~ 1 m in diameter. A moderate gain is also expected to avoid extreme pointing requirements. In addition, the system will support a low downlink data rate and no/or minimum uplink capabilities. Significant dual band coverage with both, X- and Ka- frequency bands, will be used in order to compensate for the effect of interplanetary and solar plasmas and the Earth's atmosphere.

Spacecraft navigation capabilities

It is expected that the effect would be smooth within the mission operational heliocentric distance, so that the spatial resolution of measurements and hence the up-links can be discrete. The current estimates suggest that 100 data points per month will be sufficient to provide the needed accuracy. This can be provided with a few Kbits data rate, which is standard for many existing radio-communication systems. The measurement may use a precision radio tracking, including both Doppler and range capabilities, in combination with precision determination, monitoring, and possible compensations of non-gravitational forces acting on the flight system.

The experiment may have to be complemented by additional payload elements to determine external non-gravitational forces acting on the craft (or alternatively, on the inertial reference mass). This can be accomplished by using a DC accelerometer, additional inertial reference masses, ancillary active drag-free control, and environmental sensors. The use of these additional instruments might lead to a more accurate orbit determination for the precision formation flying approach chosen for the flight system. The spacecraft design can be engineered to allow accurate control of on-board generated disturbances (i.e. thrusters-induced thermodynamics, gas leaks, other thermo- and radio-emissions, and change of optical properties of the surface, charging, or appearance of dynamical asymmetries of any sort).

Navigation relative to inertial subsatellite

Between the primary craft and the subsatellite, laser or radar tracking will be used. In this regard, both spin-stabilization and 3-axis-stabilization have their advantage and disadvantages for the mission, and further study will decide which is to be preferred. This will determine the

exact design of the laser or radar system. The relative angle determination between the main link to Earth and the local link to the subsatellite needs to be sufficiently accurate, say at a μrad level for the position knowledge and $\sim \mu$rad/s for the drift. This will allow for redundant noise cancellation in the primary craft trajectory that would ultimately lead to noise elimination from the signal by additional use of the stable clock on-board.

At a minimum, the following measurements will be required for the mission point-to-point, scalar range between one pair of spacecraft; inertial attitude and inertial rate information for each spacecraft; time tag associated with all data using the local spacecraft clock; time offset knowledge of each spacecraft clock with respect to a common time source; and comparable measurements computed from a model or directly from one of the other sensing technologies on-board. Analytical and prototype models for the sensors (i.e., models of engineering sensors) must be validated through the use of flight data.

This formation flying concept to explore the Pioneer Anomaly will lead to a validation of the ability to tightly control inter-spacecraft ranges and inertial attitudes. The technology development for this approach would contribute to the objective of continuous and collaborative control the inter-spacecraft range and inertial attitude (relative orientation) of multiple spacecraft flying in formation over long durations of time, using inter-satellite communication devices.

Chapter 3

Phased-array radar

3.1 Introduction

Since the World War II, the principles of a technique called *phased array* are known. However, the phased arrays came into operational use late in the sixties because of the needed technology improvement in fast phase shifters. An "antenna array" is a configuration of individual radiating elements that are arranged in space and can be used to produce a directional radiation pattern. Unlike mechanically-scanned antennas, the field of view is scanned electronically by inducing either a phase shift or a time delay between adjacent antenna elements. This ability to scan the field of view without moving parts, which would introduce additional noises on the mother craft, is very convenient for the purpose of the mission described above and we give, in this chapter, the appropriate specifications for it.

3.2 Principles

3.2.1 Overview

With phased array radars, the beam steering can be achieved, typically within 10 to 100 microseconds, to any point in the field of view [8]. Single-element antennas have radiation patterns that are broad and hence have a low directivity that is not suitable for long distance communications. A high directivity can be still achieved with single-element antennas by increasing the wavelength and hence the physical size of the antenna. Usually, arrays consist in identical antenna elements in a linear configuration. The radiating pattern of the array depends on this configuration, the distance between the elements, the amplitude and phase excitation of the elements, and also the radiation pattern of individual elements.

3.2.2 Definition of parameters

To estimate the best specifications of the radar required, it is useful to remind the definitions of some parameters.

Resolutions

Like any other kind of radar, the accuracy in distance of the phased-array radar depends on the bandwidth of the signal transmitted. From the signal theory, we have the following formula for the nominal range accuracy [8]

$$\Delta r = \frac{c}{2B} \, , \tag{3.1}$$

where Δr, c and B are respectively the accuracy in range, the velocity of light and the bandwidth of the signal. Consequently, an accuracy of 1 cm requires at least a bandwidth of **15 Ghz**. For

the angular resolution, the limitation comes from the beam divergence (θ_{3dB}) which is a function of the wavelength and the aperture size

$$\theta_{3dB} = \frac{1.22\lambda}{d} \,, \tag{3.2}$$

where θ_{3dB} is the 3dB-beamwidth, λ the wavelength and d the aperture diameter.

Radiation power density

Radiation power density (W_r) gives a measure of the average power radiated by the antenna in a particular direction and is obtained by time-averaging the Poynting vector. Its value is given by

$$W_r(r,\theta,\varphi) = \frac{1}{2}[E \times H^*](\text{Watts/m}^2) \,, \tag{3.3}$$

where E and H are respectively the electric and the magnetic field intensity.

Radiation intensity

Radiation intensity U in a given direction is the power radiated by the antenna per unit solid angle. It is given by the product of the radiation density and the square of the distance r

$$U = r^2 W_r \,(\text{Watts/angle}) \,. \tag{3.4}$$

Radiation pattern

The radiation pattern of an antenna can be defined as the variation in field intensity as a function of position or angle. The typical radiation pattern of an anisotropic radiator, shown below in Fig. 3.1, consists of several lobes. One of the lobes has the strongest radiation intensity compared to other lobes. It is referred to as the major lobe. All the other lobes with weaker intensity are called minor lobes. The width of the main beam is quantified by the Half Power Beamwidth (HPBW), which is the angular separation of the beam between half-power points.
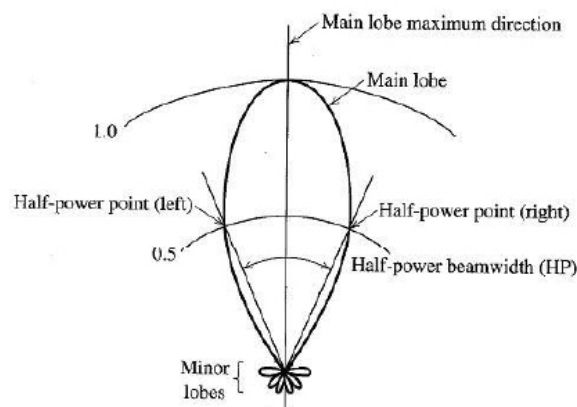

Figure 3.1: Radiation pattern.

Total power

The total power radiated by the antenna is given by

$$P_{tot} \quad = \quad \int_0^{2\pi} \int_0^{\pi} W_r(r, \theta, \varphi) r^2 d\theta d\varphi \tag{3.5}$$

$$= \quad \int_0^{2\pi} \int_0^{\pi} U(\theta, \varphi) d\theta d\varphi \,. \tag{3.6}$$

Directivity

The directive gain (D_g) in one direction is equal to the ratio of the radiated intensity in one direction to radiation intensity in all direction, i.e.

$$D_g = \frac{4\pi U(\theta, \varphi)}{P_{tot}} \,. \tag{3.7}$$

The directivity is the maximum value of the directive gain for a given direction, i.e.

$$D_0 = \frac{4\pi U_{max}(\theta, \varphi)}{P_{tot}} \,, \tag{3.8}$$

where U_{max} is the maximum radiation intensity.

3.2.3 Linear array

To start with, let us consider a linear array of two elements shown in Fig. 3.2 below. The elements are placed on either sides of the origin at a distance $d/2$ from it.
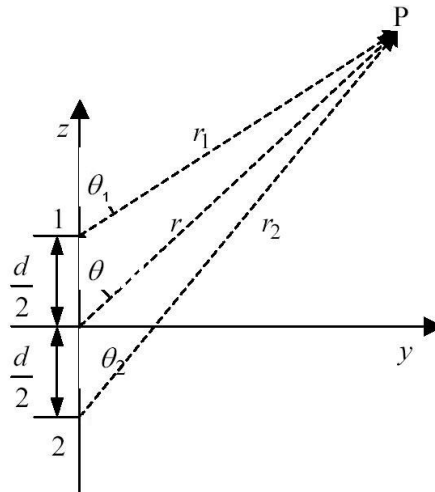

Figure 3.2: A two-element linear array.

The radiated electric fields radiated by these two elements in the far field region at point P have the following form [13]

$$E_1 \quad = \quad w_1 f_1(\theta_1, \varphi_1) \frac{e^{-j(kr_1 - \frac{\beta}{2})}}{r_1} \tag{3.9}$$

$$E_2 \quad = \quad w_2 f_2(\theta_2, \varphi_2) \frac{e^{-j(kr_2 + \frac{\beta}{2})}}{r_2} \,, \tag{3.10}$$

where

14

- w_1, w_2 are the weight, i.e. the magnitude of the current;

- f_1, f_2 are the normalized field patterns for each antenna element;

- $r1$, $r2$ are the distances of element 1 and element 2 from the observation point P;

- β is the phase difference between the the two array elements;

By considering that P is far from the array, one can make the far field approximation and the above figure can be re-drawn as shown in Fig. 3.3.
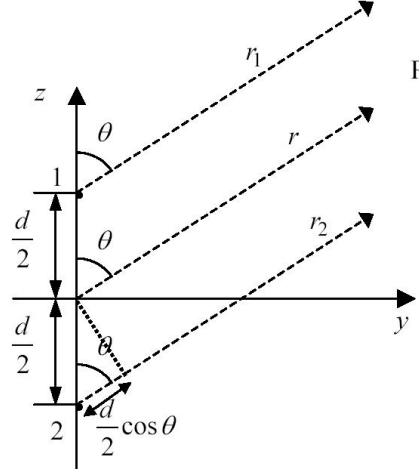

Figure 3.3: Far-field geometry of a two-element linear array.

If we assume identical array elements, the normalized field patterns are the same and the total electric field on P can be written as

$$
\begin{aligned}
E_p &= E_1 + E_2 \\
&= \frac{e^{-jkr}}{r} f(\theta, \varphi)[w_1 e^{j(k\frac{d}{2}\cos\theta + \frac{\beta}{2})} + w_2 e^{-j(k\frac{d}{2}\cos\theta + \frac{\beta}{2})}].
\end{aligned}
\tag{3.11}
$$

And finally, for uniform weighting, one has

$$
w = w_1 = w_2
\tag{3.12}
$$

$$
E_p = 2w\frac{e^{-jkr}}{r} f(\theta, \varphi) \cos(\frac{kdcos\theta + \beta}{2}).
\tag{3.13}
$$

The above relation is referred to the pattern multiplication which indicates that the total field of the array is equal to the product of the field due to the single element located at the origin and a factor called array factor, AF equal to

$$
AF = 2cos(\frac{kd\cos\theta + \beta}{2}).
\tag{3.14}
$$

These considerations lead to the following rule, true only for identical array elements

$$E_{total} = [E(\text{single element at reference point})] \times [\text{array factor}]$$

Therefore from the above discussion it is evident that the AF depends on the number of elements, the geometrical arrangement, the relative excitation magnitudes and the relative phases between elements.

3.2.4   Uniform linear array

In this section, the results of two-element array are extend to a N-element uniform linear array. The uniform linear array shown in the Fig. 3.4 consists of N elements equally spaced at distance d apart with identical amplitude excitation. There is also a progressive phase difference of β between the successive elements.
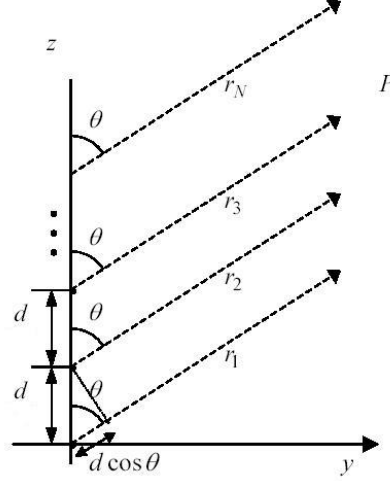

Figure 3.4: Far-field geometry of N-element array (isotropic elements along z-axis).

Let us assume that the phase of the wave arriving at the origin is set to zero and that the point P is in the far field region. The array factor of an N-element linear array of isotropic sources can be written as

$$
\begin{aligned}
AF &= 1 + e^{j(kd\cos\theta+\beta)} + e^{j2(kd\cos\theta+\beta)} + ... + e^{j(N-1)(kd\cos\theta+\beta)} \\
&= \sum_{n=1}^{N} e^{j(n-1)(kd\cos\theta+\beta)} \\
&= \sum_{n=1}^{N} e^{j(n-1)\psi} \,,
\end{aligned}
\tag{3.15}
$$

where $\psi = kd\cos\theta + \beta$. Therefore by varying β the array factor of the array can be controlled. The above AF relation can be expressed in a closed form, which is more convenient for pattern analysis,

$$
AF.e^{j\psi} = \sum_{n=1}^{N} e^{jn\psi}
\tag{3.16}
$$

$$
AF.e^{j\psi} - AF = e^{jN\psi} - 1
\tag{3.17}
$$

$$
AF = \frac{e^{jN\psi} - 1}{e^{j\psi} - 1} \,.
\tag{3.18}
$$

The last relation can be transformed as

$$
AF = e^{j\frac{N-1}{2}\psi} \frac{\sin\frac{N\psi}{2}}{\sin\frac{\psi}{2}} \,.
\tag{3.19}
$$

16

In this equation, the first term $(e^{j\frac{N-1}{2}\psi})$ is equal to one if the origin coincides with the center of the array. Therefore, neglecting that term the array factor can be re-written as

$$AF = \frac{\sin\frac{N\psi}{2}}{\sin\frac{\psi}{2}} \, . \tag{3.20}$$

3.2.5 Broadside array

An array is referred to a broadside array when it has a maximum radiation in the direction perpendicular to the axis of the array, i.e. when $\theta = 90$, as shown in Fig. 3.5. From Eq. 3.20, the maximum of the array factor would occur when

$$\psi = kd\cos\theta + \beta = 0 \tag{3.21}$$

Then $\theta = 0$ occurs when $\beta = 0$ and we have the following radiation pattern
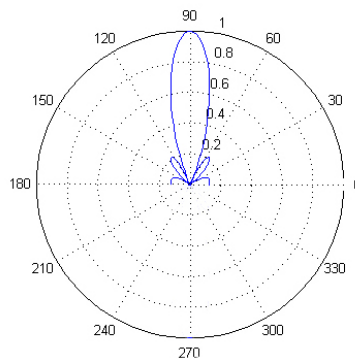

Figure 3.5: Array factor of a 5-element uniform amplitude broadside array.

Therefore, a uniform linear array will have maximum radiation in the broadside direction when all the array elements will have the same phase excitation.

3.2.6 End-fire array

An array is referred to an end-fire array when it has a maximum radiation in the direction along the axis of the array, i.e. when $\theta = 0°$ (as shown in Fig. 3.6) or $\theta = 180°$. To have this configuration, Eq. 3.20 requires $\beta = -kd$ for $\theta = 0$ and $\beta = kd$ for $\theta = 180°$.
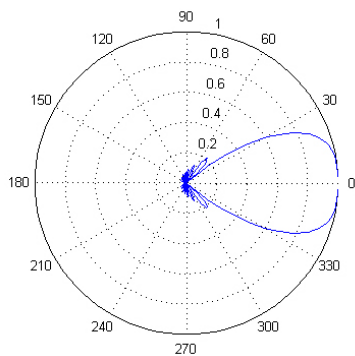

Figure 3.6: Array factor of a 5-element uniform amplitude end-fire array.

Let us now illustrate the dependence of the uniform linear array factor on the different parameters including the number of elements N and element spacing d as a function of wavelength λ.
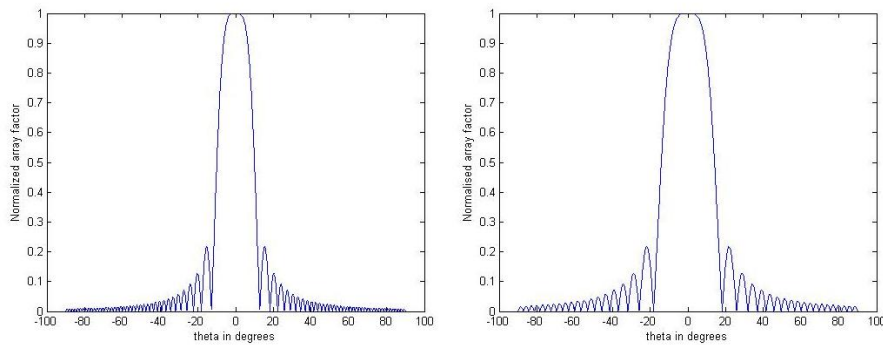
Figure 3.7: plots of the array factor plots for $d = 4\lambda$ on the left and $d = \lambda$ on the right when N=20.

The following plots of the array factor in (see Fig. 3.8) shows that the beamwidth is not only dependent on the element spacing d but also on the number of elements. From the plots, one can see that the beamwidth decreases as the number of elements in the array increases. Note that the element spacing is kept constant in both cases.
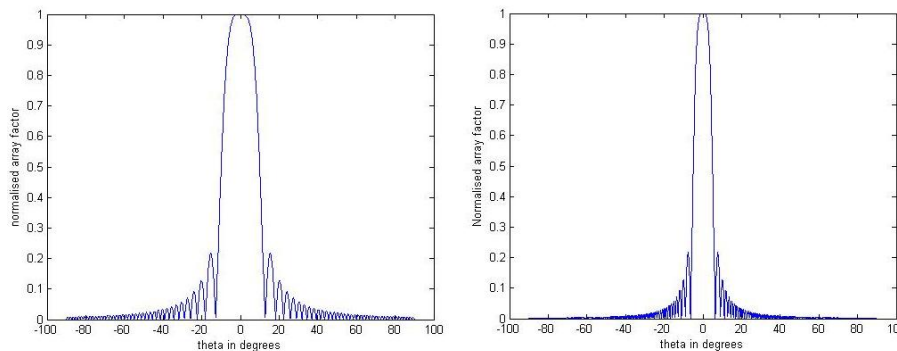
Figure 3.8: Array factor plots for N=10 on the left and N=40 on the right for $d = 4\lambda$.

Finally, note that the beamwidth remains the same if the number of elements is increased and the element spacing decreased by the same amount.

3.2.7 Phased array

The above discussion on broadside array and end-fire array indicates that the direction of the radiation for the main lobe depends on the phase difference β between the elements of the array. In the same manner, it is possible to continuously steer the main beam in any direction by varying the progressive phase β between the elements. This type of array, where the main lobe is steered to the desired direction, is referred to a phased array or a phase-scanned array.

The array factor for an N-element linear array with uniform spacing is given by,

$$AF(\theta) = \sum_{n=0}^{N-1} w_n e^{jknd\cos\theta} \, . \tag{3.22}$$

The phase β is adjusted by including a phase factor $e^{jknd\cos\theta_0}$ in the weight associated with individual element. If the steering angle desired is θ_0, the phase excitation β must be adjusted such that, when $\theta=\theta_0$,

$$\psi = kd\cos\theta + \beta = kd\cos\theta_0 + \beta = 0 \, . \tag{3.23}$$

This equation leads to

$$\beta = -kd\cos\theta_0 \, , \tag{3.24}$$

and the array factor becomes

$$AF(\theta) = \frac{sin(N\pi\frac{d}{\lambda}(\cos\theta - \cos\theta_0))}{sin(\pi\frac{d}{\lambda}(\cos\theta - \cos\theta_0))} \, . \tag{3.25}$$

Fig. 3.9 below shows a linear and a polar plot, which illustrate the above discussion. In this example, the beam is steered to an angle of 75 degrees for a 15-element array (the elements are spaced by $d = \lambda/2$).
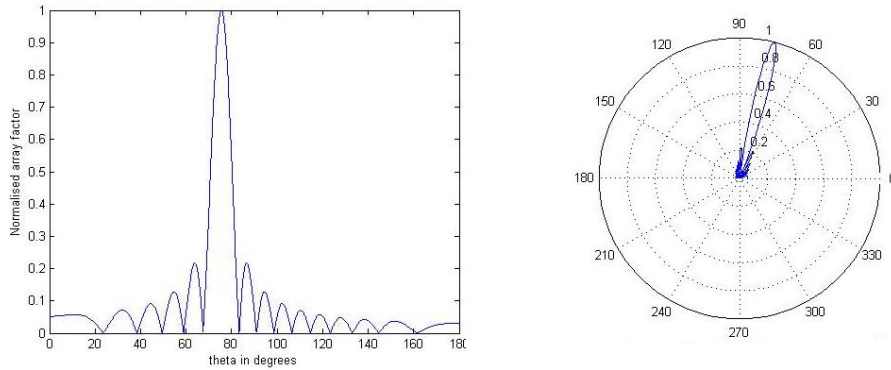

Figure 3.9: Linear and polar plots of the array factor when the beam is steered to 75 degrees.

This concept would be useful for the mission in order to keep the test mass in the field of view. Note that several test masses could be followed by a phased array radar.

3.3 Applications

The main reason to choose the phased array technique in radar is that the beam of the antenna can be steered in a certain new direction which is very much differing from its current position without delay due to mechanical inertia. This might be called "beam agility".

Figure 3.10: EMPAR on US navy ships.

This beam agility can also be important when the radar has multiple functions to be performed simultaneously. This capability is very useful for the army buildings and very widespread. In Fig. 3.3, the EMPAR multi-function phased array radar is shown. It provides fire control for the missile system for the Navy ships and it is adapted for weather detection. This may help to provide earlier warnings for tornadoes and other hazardous weather.

The technique is also used in radio astronomy in order to create the very large apertures needed. The angular resolution is established by synthesizing the direction of arrival from this aperture.

Usually, the phased array radars have the following characteristics:

- limited volume search, with waveforms dedicated to classes of objects (e.g. missiles, ships, helicopters,...).

- accurate tracking of objects.

- identification waveforms, requiring relatively long dwell time in a certain angular sector.

The order of magnitude of the antenna dwell time in a certain direction may vary from less than 1 msec to more than 100 msec. Phased array radars can be controlled to spend their time and power resources in a user defined optimum way. This is not the case with the common surveillance or track radar, which are optimized for one particular mission only. Managing the radar so that it complies with its operational objectives, leaving no time and no power unspent is a very complex task. The beam agility is just one aspect of the complexity of the design, introduced by the multifunction capability. It is one of the cost drivers, making that phased array radars cost multiple tens of millions of dollars per system.

There is one other cost driver: the antenna. Either it is the power distribution network and phase shifting capability or the transmit/receive module which is pushing the cost very high. Current cost of T/R modules at X-band is in the order of 1000 euros a piece, where the expectation is that it will lower to 500 euros once mass production can be realized. Note that one phased array is normally populated by 1000 to 3000 of these T/R modules per array.

Given this cost factor, it should be no surprise that the majority of technology actions concerns either reduction of the cost by technology evolution or by technology substitution. The complexity however remains.

3.4 For the mission

3.4.1 Specifications

In Table 3.1 below, the key parameters of phased array radars designed for the Mars Science Laboratory (MSL) mission are shown [9]. The column A shows the characteristics of a phased

array radar designed with the technology of 2002 while the column B shows the specifications that will be possible to have on MSL for its launching date (2009). MSL is a NASA mission aimed at studying Mars with very high-performance remote sensing technology. The phased array radar onboard will be used for the landing by targeting a pre-selected site of scientific interest as soon as the lander will be at an altitude of 9 km.

Parameter	Units	A	B
Center frequency	GHz	35	94
Wavelength	mm	8.57	3.19
Antenna Size	m^2	1.3×1.3	0.5×0.5
Element Beamwidth	deg	16.8	15.2
Array Beamwidth	mrad	7.9	7.7
Power per Element	dBm	10.0	10.0
Number of Elements	-	128	128
Total Transmit Power	dBm	31.1	31.1
Element Noise figure	dB	5.0	8.0
System Noise Bandwidth	Ghz	1.0	1.0
Number of Frequency Hops	-	5	5
Noise Equivalent σ_0(9000m)	dB	-24.5	-22.5
Noise Equivalent σ_0(500m)	dB	-42.6	-27.6
Estimated System Mass	kg	29.3	29.9
Estimated System Power	W	206	246

Table 3.1: Key radar parameters.

These values allows us to estimate the specifications of a phased array radar, which will track the test mass in the mission. To do this, we suppose a realistic requirement of 1 degree on the angular resolution. This gives us a constraint of 20 cm on the minimum length of the antenna (for the case B). Table 3.2 below shows the estimated specifications using the case B.

Output Power	Input Power	Size	Mass	Pointing	Field	Accuracy
60 mW	20W	20x5cm^2	13kg	1°	23°	10cm

Table 3.2: Estimated parameters for the phased array radars.

A recent study at JPL has shown the feasibility of a G-band (140-220 GHz) phased array radars beyond 2012. They expect to increase the accuracy by a factor of 2 or 3 while simultaneously decreasing the antenna size by a factor of 2 [11].

3.4.2 Requirement on the test mass

In the previous section, we have estimated the specifications of a phased array radar in order to have 10 cm for the accuracy in distance and 1 degree for the angular resolution. However, this radar is not perfect and enough power has to be received from the test mass in order to detect a signal. This means that the signal-to-noise ratio has to be sufficiently high. The typical value for maximum sensitivity of a phased array radar is -94dBm [8]. For a given size of the test mass, this value leads to a constraint on the maximum distance between the mother craft and the test mass. This distance can be calculated using the figure below
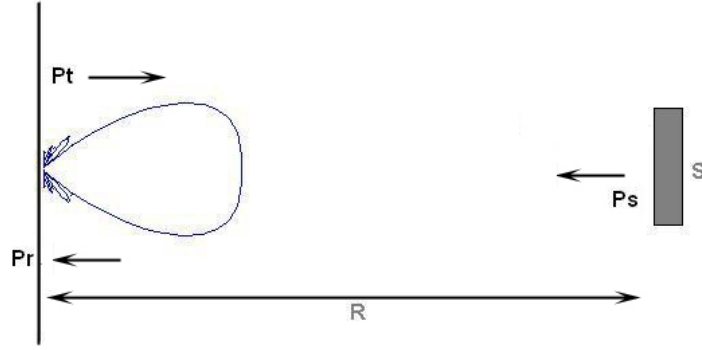
Figure 3.11: Configuration geometry.

By the conservation of energy, the power by square-meter at the distance R from the mother craft is given by [12]

$$E_r = \frac{P_t G}{4\pi R^2}, \qquad (3.26)$$

where P_t is the power transmitted and G the gain of the antenna. Therefore, the power emitted by the test mass can be written as

$$P_s = E_r S\sigma = \frac{P_t G}{4\pi R^2} S\sigma, \qquad (3.27)$$

where σ is the reflectivity of the test mass and S its surface. Finally, the part of the power reaching the antenna is given by

$$P_r = \frac{P_s}{4\pi R^2} A = \frac{P_t G}{(4\pi R^2)^2} A S\sigma. \qquad (3.28)$$

To maximize the power of the signal received, a high-reflective material will cover the test mass. At frequencies close to 100 GHz, good choices would be carbon fiber or a thin layer of vacuum-deposited aluminium, which are usually used for the high frequency antennas reflectors. In the following, we assume a perfect reflective test mass, i.e. $\sigma = 1$.

Finally, Eq. 3.28 can be simplified as

$$P_r = 4.10^4 \frac{A^3 S}{R^4}, \qquad (3.29)$$

using the following considerations

1. The gain of the antenna depends on its size and its center frequency like:

$$G = \frac{4\pi A f^2}{c^2}, \qquad (3.30)$$

   where f is the center frequency and c the velocity of the light.

2. The power transmitted is directly proportional to the number of elements and thus, to the surface of the phased array radars. In Table 3.2, we can see that the power transmitted by one element (about 20 cm^2) is equal to 10.0 dBm (=10mW). Therefore, it is easy to have the relation between these two quantities.

In the figure below, the maximum distance of the test mass is shown as a function of the size of the test mass.
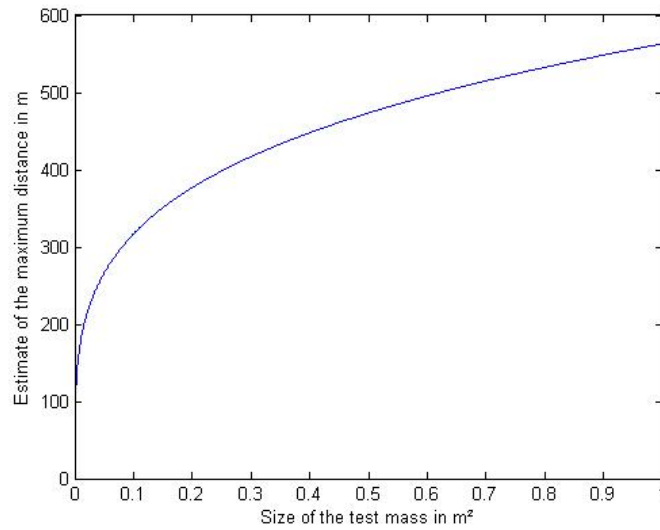

Figure 3.12: Maximum distance between the mother craft and the test mass as a function of the surface of the test mass seen by the mother craft.

If we assume a realistic value of 0.05 m^2 for the surface of the test mass, one can see that in order to have enough power received at the radar, the distance cannot be higher than 250 m. Unfortunately, the present design of the mission needs the test mass to be tracked till few kilometers. By keeping unchanged the size of the test mass, this can be done by increasing the number of elements of the phased array radars and therefore, this leads to new specifications. By using Eq. 3.29 and Table 3.2, one can draw the figure below that shows the power consumption of the MSL's phased array radar as a function of the maximum tracking distance.
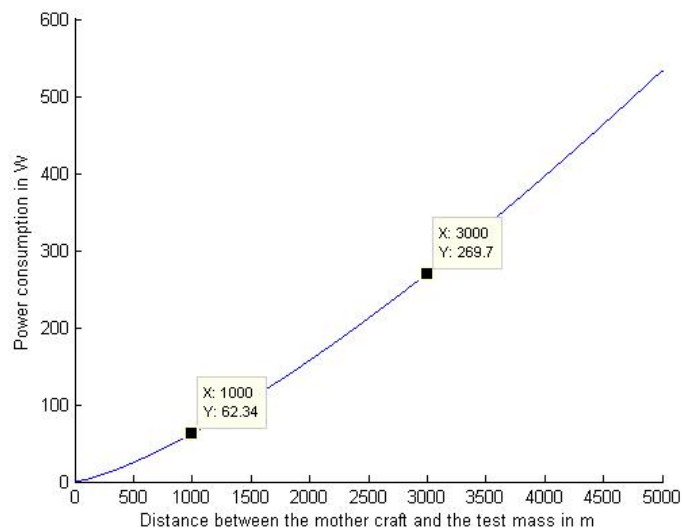

Figure 3.13: Power consumption as a function of the maximum tracking distance.

Finally, the specifications of a phased array radar that can track a 0.05 m^2 disk-shaped test

mass are

Distance	Frequency	Output Power	Input Power	Size	Mass	Pointing	Accuracy
1 km	94 GHz	0.33W	60W	$0.06m^2$	7kg	$0.4°$	10cm
3 km	94 GHz	1.3 W	240W	$0.24m^2$	29kg	$0.4°$	10cm

Table 3.3: New Estimate for the parameters of the phased array radars.

From these results, we conclude that the power necessary to track a test mass located at 3 km from the mother craft with the accuracy required, would be about 240 W, which is comparable to the power budget of the whole mission. For a test mass located at 1 km from the mother craft, which is roughly the minimum distance to avoid too large perturbations from the mother craft, the power consumption would be about 60 W. This is much bigger than the 10 mW required by the laser system. The mass of a radar system would also be much bigger than the mass of a laser system. Hence the radar tracking system have to be considered as a backup option for the mission.

Chapter 4

Outcomes of the workshop

The first outcome of the meeting is related to the progress made about dust concentration in the outer Solar System and its eventual influence on the deceleration of the spacecraft. From the results of recent analytical and experimental work reported on the meeting, substantial influence from grain dust can be excluded to explain the Pioneer anomaly. It was also discussed the gravitational forces eventually induced by a number of speculative larger objects in the range 20 to 25 AU, which could explain the Pioneer anomaly. But also larger objects at this relatively short distance from the Sun are unlikely and must be excluded with respect to recent system models and recent observations.

It was also reported by the US people on present activities for more analytical work with the Pioneer data. There is some funding to transfer the data from the old magnetic tapes to DVDs. This work is strongly supported by Tom Prince, the JPL Chief Scientist and will start in April. Additional activities for enhanced data analysis is proposed to JPL's management, and there is a major interest of JPL to involve European scientists. Also, the US Planetary Society just released a Public Appeal in order to raise money for the analysis of the Pioneer data. US people hope to have the Pioneer anomaly work featured in the new NASA roadmap to be published end of summer 2005.

Concerning the dedicated-mission to the Pioneer anomaly, the meeting was productive to enhance and update the characteristics of the mission. The characteristics are shown in the following tables.

A. Payload design

1	Test mass design			
1.1	shape		sphere	disk
1.2	size (radius)		10 cm	20 cm
1.3	mass		10 kg	20 kg
1.4	distance from mother craft	min	200 m	200 m
		max	5 km	5 km
1.5	release mechanism			
		mass	5 kg	10 kg
		size	12 cm	24 cm
		position	on the rotation axis	
1.6	stabilization		rotation	
2	Design of inter-spaceraft tracking			
2.1	LASER vs RADAR		LASER	RADAR
		output power	1 mW	0.33 W
		input power	10 mW	60 W
2.2	overall design			
		size	10 cm	0.06 m²

	mass	7 kg	20 kg
	pointing	urad	mrad
	field of view	10 deg	45 deg
	beam divergence	urad	1 deg
	duty cycle	msec	5sec
	accuracy	1 cm	10 cm
2.3	attitude control (star scanner)		
	pointing accuracy	mrad	
	pointing stability	mrad/sec	
3	Ground tracking		
3.1	range	3 m	
3.2	velocity	0.03 mm/s	
4	Additional instrumentation		
4.1	dust-analyzer (mass/p	1 kg / 0.5 W	
4.2	gas-analyszer	0.5 kg / 1 W	
4.3	plasma-analyzer	2 kg / 1 W	
4.4	heat and inertial design	<10E-8cm/s²	

Table 4.1: Test mass and inter-spacecraft designs.

We also discussed on the Solar radiation pressure on the test mass, the coulomb forces and the noise introduced by the use of a spring as release mechanism.

B. Spacecraft design

1	Main spacecraft			1.4	power subsystem options	3 RTGs	
1.1	power budget	200 W		2	Mission analysis		
1.2	mass budget	250 kg		2.1	propulsion system	hydrazine	
1.3	communication requirements			2.2	launch mass and configuration	500 kg	
	frequencies	Ka / X		2.3	launch option	direct/Jupiter gravity assist	
	comm. rate	500 bps		2.4	Launcher	Ariane 5 / Proton	

Table 4.2: Spacecraft design and mission analysis.

The possibility to use Solar sail propulsion was also a lot discussed at the workshop. This technology is still in its infancy, but interest in its future is high. What is needed is lighter weight material for sails. The mission to explore the Pioneer anomaly could be a good opportunity to stimulate its evolution.

C. Science objectives

The main scientific objective would be to explore the anomaly with an accuracy 3 orders of magnitude better than with the Pioneers. There are also other scientific objectives which could be incorporated in the mission. By example, it would be the opportunity to study the Solar System (magnetic field, dust,etc) and the gravitational waves.

Bibliography

[1] J. D. Anderson, P. A. Laing, E. L. Lau, A. S. Liu, M. M. Nieto and S. G. Turyshev, "Indication, from Pioneer 10/11, Galileo, and Ulysses Data, of an Apparent Anomalous, Weak, Long-Range Accelerattion," Phys. Rev. Lett. **81** (1998) 2858 [arXiv:gr-qc/9808081].

[2] J. D. Anderson, P. A. Laing, E. L. Lau, A. S. Liu, M. M. Nieto and S. G. Turyshev, "Study of the anomalous acceleration of Pioneer 10 and 11," Phys. Rev. D **65**, 082004 (2002) [arXiv:gr-qc/0104064].

[3] J. D. Anderson, P. A. Laing, E. L. Lau, M. M. Nieto and S. G. Turyshev, "Search for a Standard Explanation of the Pioneer Anomaly," Mod. Phys. Lett. A **17**, 875-885 (2002) [arXiv:gr-qc/0107022].

[4] C. B. Markwardt, "Independent Confirmation of the Pioneer 10 Anomalous Acceleration," arXiv:gr-qc/0208046.

[5] J. D. Anderson, S. G. Turyshev and M. M. Nieto, "A mission to Test the Pioneer Anomaly," Int. J.Mod. Phys. D **11**, 1545-1551 (2002) [arXiv:gr-qc/0205059].

[6] M. M. Nieto and S. G. Turyshev, "Finding the Origin of the Pioneer Anomaly," CQG **21**, 4005-4023 (2004). [arXiv:gr-qc/0308017].

[7] H. Dittus and al. (Cosmic Vision Theme Proposal), "To Explore the Pioneer Anomaly," submitted to ESA's Fundamentals Physics Advisory Group ESA Headquarters, Paris, 17 September 2004.

[8] J.M. Golio: "The RF and Microwave Handbook Rocess (Electrical Engineering Handbook series)," CRC Press (2000). Pulse Radar(M.L. Belcher and J.T. Smith).

[9] B.D. Pollard, G. Sadowy, D. Moller and E. Rodriguez: IEEEAC paper 1188(2002).

[10] P. Van Genderen: "State-of-the-art and trends in phased array radar," Netherlands Foundation for Research in Astronomy (1999).

[11] http://marstech.jpl.nasa.gov/.

[12] C.Elachi:"Introduction to the physics and Techniques of Remote sensing," Wiley,N.Y.,1987.

[13] M. Van Droogenbroeck: "Principes des telecommunications analogiques et numeriques," Universty of Liege (2005).